PNAS

www.pnas.org

Supplemental Information for

Multiple deprotonation paths of the nucleophile 3′-OH in the DNA synthesis reaction

Mark T. Gregory[1], Yang Gao[1,2,4], Qiang Cui[3] and Wei Yang[1,4]

[1] Laboratory of Molecular Biology, NIDDK, National Institutes of Health, Bethesda, MD 20892, USA

[2] Current Address, Department of BioSciences, Rice University, TX 77025

[3] Department of Chemistry, Boston University, 590 Commonwealth Ave, MA 02215

* Correspondence: weiy@niddk.nih.gov; yg60@rice.edu

This PDF file includes

1. SI Methods
2. Figures S1 to S4
3. Tables S1 and S2
4. SI References

SI Methods

Steady-State Kinetic Assay

Steady-state kinetic parameters K_M and K_{cat} were measured using the template/primer pairs shown in figure 1D. The reaction mixture contained 2.5 or 5 nM Pol η, 0-60 μM dATP, 5 μM 5´-labeled primer and unlabeled template, 40 mM Tris (pH 7.5), 5 mM $MgCl_2$, 100 mM KCl, 10 mM Dithiothreitol, 0.1 mg/ml Bovine Serum Albumin, 5% glycerol. Reactions were initiated by addition of dATP and $MgCl_2$, incubated at 22°C (room temperature) for 5 minutes, and quenched with an equal volume of 90% formamide with 10 mM NaOH and xylene cyanol. After heating at 90°C for 3 minutes and rapid cooling on ice the products were resolved on 20% poly-acrylamide gels containing 5.5 M urea, visualized using a Typhoon Trio (GE Healthcare), quantified using ImageQuantTL (GE Healthcare) software, and curve fitting was performed using Prism 5 (Graphpad) software.

Crystallization and Data Collection

For crystallization, purified Pol η and DNA were mixed in a 1:1.09 molar ratio and incubated on ice to form a binary complex. DNA sequences used are listed in supplemental Table S2. After three-fold dilution to reduce the salt concentration to 150 mM KCl, the complexes were concentrated to 3.5 mg/ml of protein (determined by the Bradford method). For static ternary-complex structures, the correct dNMPNPPs (non-reactive dNTP analogs) and 1.5 mM $MgCl_2$ were incubated with Pol η and DNA substrate. For *in crystallo* reactions, 1 mM dATP and $CaCl_2$ at equal concentration to Pol η were added to form the ternary complexes before crystallization. Crystals were obtained using the hanging drop method over a reservoir containing 0.1 M MES (pH 6.0), 1 mM DTT and 15-20% PEG 2000MME. Microseeding was used for when consistent crystal sizes were

difficult to obtain with simple vapor diffusion. For static structures crystals were soaked briefly in the stabilization buffer containing 0.1 M MES (pH 6.0), 1 mM DTT and 20% PEG 2000MME plus 20% glycerol for cryo-protection before flash cooling in liquid nitrogen. For time resolved structures, crystals were soaked in 20% PEG 2K-MME/ 0.1 M MES-KOH (pH 7.0)/ 1 mM DTT and 5 μM dATP for 30 minutes, and then transferred to the reaction buffer containing 20% PEG 2K-MME, 0.1M MES-KOH (pH 7.0), 1 mM DTT and 1 mM $MgCl_2$ for various time length as indicated then briefly dipped in the reaction buffer with 20% glycerol for cryo protection prior to freezing in liquid nitrogen. Diffraction data were collected at 100K on the 22BM beamline at the Advanced Photon Source (APS).

Structure Determination

Diffraction data were processed with HKL2000 or XDS and reduced to structure factors using TRUNCATE (1-4). All crystals were in the P61 space group, and all structures isomorphic with that of Pol η complexed with normal DNA substrate and dAMPNPP (PDB code 3MR2), which provides phase information. Models were built in COOT and refined in PHENIX (5, 6). Data collection and refinement statistics are summarized in Table S1. All structural figures were prepared with PyMol (7).

Molecular Dynamics Simulations

Classical molecular dynamics (MD) simulations were carried out with explicit solvent molecules under physiological salt (150 mM NaCl) condition. Simulations were conducted for the WT enzyme with the dT- (PDB: 5KFG) as well as dA-primer, and S113A with both dA- and rA-primers; the incoming nucleotide was dATP in all cases. The starting structures were based on the relevant crystal structures for the reactant (RS) configuration and fully solvated. Because the C-site Mg^{2+} is necessary for catalysis (8), it

was modeled next to the α-phosphate of dATP according to the PS structure observed after 100 s in the *in crystallo* reaction time course. For S113A, simulations started with the primer end adopting either the C2'-endo or C3'-endo puckering mode as observed in the crystal structures. Moreover, simulations were performed with and without the WatN near the 3'-OH group, which is not always observed in the *in crystallo* reactions; simulations were also performed to test the impact of the Arg61 sidechain orientation, as multiple orientations have been observed in the crystal structure. Overall, 4 and 9 sets of independent simulations were performed for WT and S113A, respectively, with each simulation lasting between 50 ns to 100 ns.

The simulations were set up using the standard periodic boundary condition with CHARMM-GUI (9). The initial simulation box length was 107 Å and reduces to about 104 Å following NPT equilibrations; the number of atoms is approximately 115,000. The protein, nucleic acids, incoming nucleotide, water and salt ions were treated with the CHARMM 36m force field (10-12). Electrostatic interactions were treated with particle-mesh-Ewald (13) with a grid size of ~1 Å and a real-space cut-off of 12 Å, and van der Waals interactions were treated with a shift scheme with the shift and cut-off distances of 10 and 12 Å, respectively. SHAKE (14) was used to constrain all bonds involving hydrogen, allowing an integration time step of 2 fs. The system was first minimized with steepest descent for 5000 steps and then equilibrated with NVT simulations for 125 ps using the Langevin thermostat (γ=1 ps^{-1}) at 303 K. Production runs (between 50 ns and 100 ns for each set up) were carried out in the NPT ensemble with the Langevin thermostat and the Monte Carlo barostat (p=1 bar). Configurations were saved every 100

ps for analysis. All simulations were conducted with OpenMM7.2, (15) and analyses have been carried out using CHARMM45 (16).

Supplemental Figures

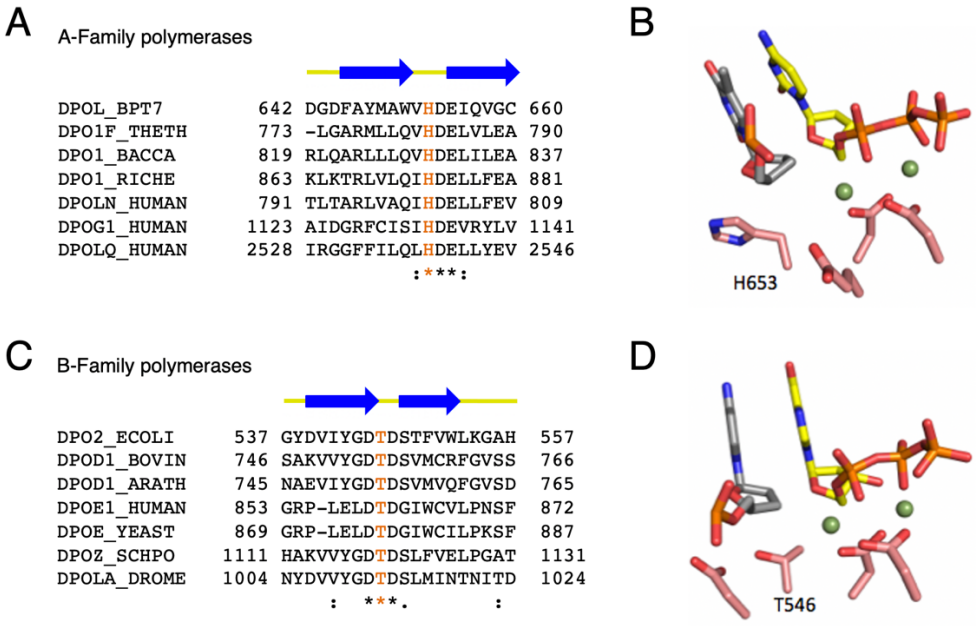

Fig. S1. The equivalent residue of S113 is conserved in A- and B- family DNA polymerases. (*A*) Alignment of active site residues within motif III of the A-family polymerases. Bacteriophage T7 Pol (DPOL_BPT7, P00581), T. *thermophiles* Pol I (DPO1F_THETH, P30313), B. *caldotenax* Pol I (DPO1_BACCA, Q04957), R. *Helvetica* Pol I (DPO1_RICHE, Q9RLB6), H. *sapiens* Pol ν (DPOLN_HUMAN, Q7Z5Q5), H. *sapiens* Pol G1 (DPOG1_HUMAN, P54098), H. *sapiens* Pol Q (DPOLQ_HUMAN, O75417). (*B*) The active site of T7 DNA polymerase complexed with DNA (dideoxy primer) and dCTP in the presence of two Mg^{2+} (green sphere) (PDB: 1T8E). (*C*) Alignment of the B-family polymerases includes: E. *coli* Pol II (DPO2_ECOLI, P21189), B. *taurus* Pol δ (DPOD1_BOVIN, P28339), A. *thaliana* Pol δ (DPOD1_ARATH, Q9LVN7), H. *sapiens* Pol ε (DPOE1_HUMAN, Q07864), S. *cerevisiae* Pol ε (DPOE_YEAST, P21951), S. *pombe* Pol ζ (DPOZ_SCHPO, Q9P6L6), D. *melanogaster* Pol α (DPOLA_DROME, P26019). The residue spatially and functionally equivalent to S113 of human Pol η is highlighted in red in each polymerase. (*D*) The active site of *E. coli* DNA polymerase II complexed with DNA (dideoxy primer) and dGTP in the presence of two Mg^{2+} (green sphere) (PDB: 3MAQ).

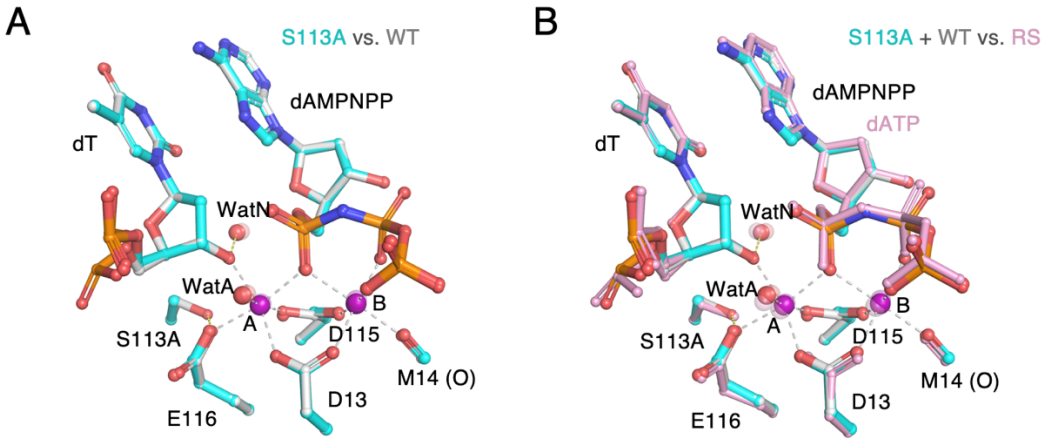

Fig. S2. The static structures of dAMPNPP are superimposable with the RS structures. (A) Structure superposition of WT and S113A active sites. Both WT (silver sticks) and S113A (cyan sticks) are complexed with a dT-primer and dAMPNPP. Mg^{2+} coordination is indicated by grey dashes. Hydrogen bonds are shown as yellow dashes. Water molecules bound to the 3′-OH (WatN) and A-site Mg^{2+} (WatA) are conserved in all these structures. (B) Superposition includes the reactive-state (RS) structure of WT Pol η complexed with a dT-primer and dATP at 40s after Mn^{2+} exposure (PDB: 5KFG), which is shown in semi-transparent pink.

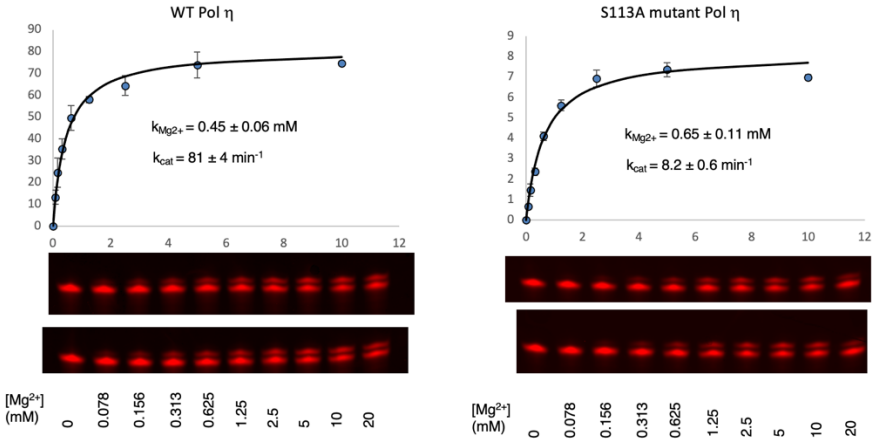

Fig. S3. The Mg^{2+} concentration dependence of WT and S113A mutant Pol η. Each reaction contained 5 nM WT or 50 nM S113A Pol η, 5 μM DNA, 100 μM dATP, and $MgCl_2$ varied between 0.078-20 mM and was carried out at 37°C for 5 min. Raw data are shown under the kinetic profiles. Because at 20 mM Mg^{2+} exhibited inhibitory effect, the 20 mM data point is excluded in the kinetic data fitting.

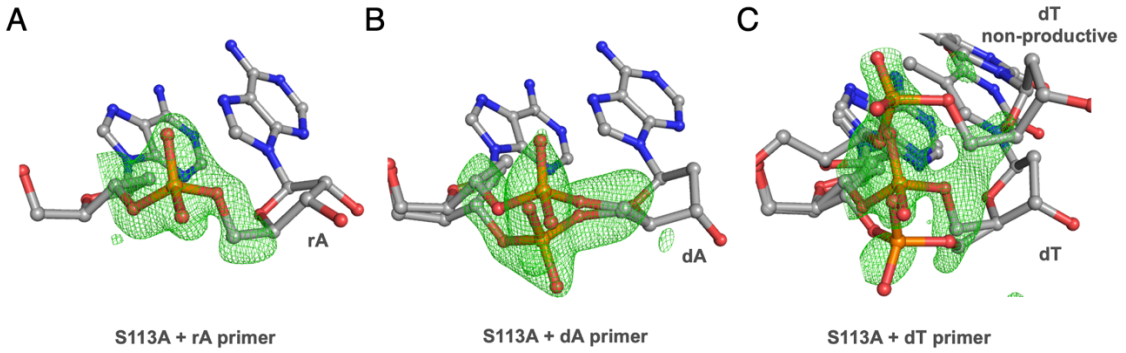

Fig. S4. Conformations of the phosphate group at the primer 3′-end. A. The structure of S113A Pol η with the rA-primer at t=0s. B. The equivalent structure of S113A Pol η with the dA-primer at t=0s. C. S113A Pol η with the dT-primer at t=0s. The last two nucleotides at the primer 3′-end are shown in grey sticks. Each Fo-Fc map with the phosphate group omitted is contoured at 3σ and superimposed as green mesh. The phosphate group of the rA-primer is in a unique conformation, while it has two conformations in the dA- or dT-primers. In addition, a non-productive conformation of the last nucleotide exists in the dT-primer structure.

Table S1. Statistics of data collection and structure refinement

(A) Static structures of WT Pol η-DNA-dAMPNPP ternary complexes

	WT+dA	WT+rA	WT+2´-Fl-dA	WT+dT+0.1mM dAMPNPP
PDB Code	7M7L	7M7M	7M7N	7M7O
Data collection				
Space group	$P6_1$	$P6_1$	$P6_1$	$P6_1$
Cell dimensions				
a, b, c (Å)	98.65	98.44	98.44	98.59
	98.65	98.44	98.44	98.59
	81.99	82.11	82.11	82.2
α, β, γ (°)	90, 90, 120	90, 90, 120	90, 90, 120	90, 90, 90
Resolution (Å) [1]	30-1.57	21.31-1.45	21.31-1.31	30-1.8
	(1.60-1.57)	(1.48-1.45)	(1.33-1.31)	(1.83-1.80)
R_{sym} or R_{merge} [1]	6.9 (47.7)	5.9 (56.5)	5.7 (68.9)	9.5 (71.8)
I / σI [1]	11.7 (2.9)	9.0 (1.7)	12.0 (2.0)	10.6 (1.7)
Completeness (%) [1]	99.7 (98.6)	97.6 (84.3)	96.8 (90.4)	90.7 (93.1)
Redundancy [1]	4.2 (3.3)	2.9 (1.7)	3.9 (3.5)	4.1 (4.0)
Refinement				
No. Reflections [1]	62075 (6106)	76479 (6572)	104809 (9730)	38103 (3900)
R_{work}	0.18 (0.22)	0.18 (0.28)	0.18 (0.27)	0.18 (0.25)
R_{free}	0.22 (0.25)	0.21 (0.31)	0.21 (0.28)	0.23 (0.32)
No. atoms	4428	4475	4506	4410
Macromolecules	3885	3894	3918	3927
Ligands	55	61	61	61
Solvent	488	520	527	422
B-factors	21.0	23.6	20.3	22.6
Macromolecules	20.0	22.4	19.4	21.8
Ligands	18.6	21.4	17.1	25.2
Solvent	29.1	32.2	27.5	29.3
Ramachandran				
Favored (%)	98.3	97.4	97.6	97.4
Outlier (%)	0	0	0	0
R.m.s deviations				
Bond lengths (Å)	0.006	0.007	0.005	0.010
Bond angles (°)	0.90	1.18	0.86	1.38

1. Data in the highest resolution shell is shown in the parenthesis.

(B) Static structures of S113A Pol η-DNA-dAMPNPP ternary complexes

	S113A+dA	S113A+dT	S113A+rA	S113A+dT+0.1mM dAMPNPP
PDB Code	7M7P	7M7Q	7M7R	7M7S
Data collection				
Space group	$P6_1$	$P6_1$	$P6_1$	$P6_1$
Cell dimensions				
a, b, c (Å)	98.77	98.93	98.65	98.68
	98.77	98.93	98.65	98.68
	81.84	81.81	81.74	81.83
α, β, γ (°)	90, 90, 120	90, 90, 120	90, 90, 120	90, 90, 90
Resolution (Å) [1]	31.51-1.80 (1.83-1.80)	32.38-2.26 (2.30-2.26)	23.36-1.81 (1.84-1.81)	31.5-1.85 (1.88-1.85)
R_{sym} or R_{merge} [1]	12.5 (66.1)	15.4 (68.6)	9.1 (54.4)	8.2 (62.8)
I / σI [1]	9.2 (2.5)	8.5 (2.0)	10.0 (2.0)	10.3 (2.0)
Completeness (%) [1]	98.6 (98.0)	98.3 (99.4)	97.7 (95.3)	100 (100)
Redundancy [1]	3.8 (3.8)	3.9 (3.7)	3.1 (2.2)	3.7 (3.5)
Refinement				
No. Reflections [1]	41670 (4135)	20831 (2094)	40274 (3922)	38691 (3854)
R_{work}	0.20 (0.24)	0.17 (0.23)	0.18 (0.24)	0.18 (0.27)
R_{free}	0.25 (0.31)	0.22 (0.32)	0.22 (0.30)	0.23 (0.36)
No. atoms	4444	4294	4194	4428
Macromolecules	3935	3853	3906	3967
Ligands	79	55	43	73
Solvent	430	386	245	388
B-factors	21.0	25.7	21.9	23.5
Macromolecules	20.1	25.3	21.8	22.8
Ligands	24.9	25.8	20.9	29.8
Solvent	28.5	29.6	24.3	29.4
Ramachandran				
Favored (%)	97.2	97.2	97.6	98.4
Outlier (%)	0	0	0	0
R.m.s deviations				
Bond lengths (Å)	0.009	0.011	0.008	0.006
Bond angles (°)	1.19	1.43	1.27	0.9

(C) *in crystallo* reaction of S113A Pol η with a dT-primer

	S113A+dT 0s	S113A+dT 480s
PDB Code	7M7T	7M7U
Data collection		
Space group	$P6_1$	$P6_1$
Cell dimensions		
a, b, c (Å)	98.63	98.22
	98.63	98.22
	82.02	81.73
α, β, γ (°)	90, 90, 120	90, 90, 120
Resolution (Å) [1]	26.91-1.46 (1.49-1.46)	29.48-1.94 (1.97-1.94)
R_{sym} or R_{merge} [1]	6.2 (60.6)	8.0 (48.0)
I / σI [1]	9.1 (2.0)	9.5 (3.3)
Completeness (%) [1]	99.0 (97.1)	98.4 (94.3)
Redundancy [1]	3.3 (3.1)	3.3 (2.6)
Refinement		
No. Reflections [1]	77574 (7579)	32768 (3146)
R_{work}	0.18 (0.27)	0.16 (0.21)
R_{free}	0.21 (0.31)	0.22 (0.29)
No. atoms	4651	4661
Macromolecules	4011	4016
Ligands	50	51
Solvent	590	594
B-factors	22.3	27.7
Macromolecules	21.1	26.5
Ligands	16.9	24.7
Solvent	30.5	36.2
Reaction		
Ratio of RS/PS	0.7 / 0	0.5 / 0
A-site	0.3 K^+	0.5 Mg^{2+}
A-site B-factor	19.8	32
B-site	0.7 Ca^{2+}	0.2 Ca^{2+} / 0.5 Mg^{2+}
B-site B-factor	11.3	21.7 / 21.7
Ramachandran		
Favored (%)	98.4	98.4
Outlier (%)	0	0
R.m.s deviations		
Bond lengths (Å)	0.007	0.007
Bond angles (°)	1.01	1.02

(D) *in crystallo* reaction of WT Pol η with a dA-primer

	WT+dA 0s	WT+dA 40s	WT+dA 100s	WT+dA 230s	WT+dA 300s
PDB Code	7M7Y	7M7Z	7M80	7M81	7M82
Data collection					
Space group	$P6_1$	$P6_1$	$P6_1$	$P6_1$	$P6_1$
Cell dimensions					
a, b, c (Å)	98.75 98.75 82.16	98.78 98.78 82.06	98.84 98.84 82.04	99.15 99.15 81.76	98.68 98.68 82.16
α, β, γ (°)	90, 90, 120	90, 90, 120	90, 90, 120	90, 90, 120	90, 90, 120
Resolution (Å) [1]	32.33-1.80 (1.83-1.80)	30.08-1.82 (1.85-1.82)	32.35-1.80 (1.83-1.80)	30.16-2.05 (2.09-2.05)	32.30-1.80 (1.83-1.80)
R_{sym} or R_{merge} [1]	13.1 (72.4)	11.8 (68.0)	7.9 (56.7)	9.0 (64.1)	12.6 (61.7)
I / σI [1]	10.7 (2.0)	10.1 (3.2)	13.3 (2.6)	9.9 (2.1)	11.7 (2.3)
Completeness (%) [1]	98.6 (100.0)	99.5 (98.4)	99.8 (100.0)	98.9 (99.3)	99.8 (100.0)
Redundancy [1]	3.0 (3.1)	5.4 (5.3)	4.4 (4.4)	3.8 (3.6)	3.8 (3.7)
Refinement					
No. Reflections [1]	41564 (4245)	40152 (3962)	31719 (3135)	28500 (2836)	27314 (2732)
R_{work}	0.18 (0.24)	0.18 (0.23)	0.16 (0.22)	0.17 (0.23)	0.16 (0.22)
R_{free}	0.22 (0.29)	0.23 (0.29)	0.22 (0.29)	0.23 (0.29)	0.22 (0.32)
No. atoms	4461	4424	4447	4307	4438
Macromolecules	3885	3834	3849	3900	3870
Ligands	55	66	61	61	61
Solvent	521	524	537	346	507
B-factors	26.5	23.6	29.4	37.5	28.2
Macromolecules	25.7	22.8	28.5	37.1	27.6
Ligands	21.3	19.3	23.4	35.1	22
Solvent	32.8	30.4	36.7	42.9	33.5
Reaction					
Ratio of RS/PS	1.0 / 0	0.8 / 0.2	0.6 / 0.4	0.45 / 0.55	0.35 / 0.65
A-site	-	0.5 Mg^{2+}	0.5 Mg^{2+}	0.4 Mg^{2+}	0.35 Mg^{2+}
A-site B-factor		18.8	25.7	34.6	14.5
B-site	1 Ca^{2+}	0.5 Ca^{2+} / 0.5 Mg^{2+}	0.3 Ca^{2+} / 0.7 Mg^{2+}	0.3 Ca^{2+} / 0.7 Mg^{2+}	0.3 Ca^{2+} / 0.7 Mg^{2+}
B-site B-factor	15.6	10.0 / 10.0	16.3 / 16.4	24.1 / 24.8	12.1 / 11.9
C-site	-	-	0.4 Mg^{2+}	0.55 Mg^{2+}	0.65 Mg^{2+}
C-site B-factor	-	-	30.4	38.3	26.5
Ramachandran					
Favored (%)	98.4	98.4	98.4	98.4	98.4
Outlier (%)	0	0	0	0	0
R.m.s deviations					
Bond lengths (Å)	0.01	0.012	0.008	0.008	0.006
Bond angles (°)	1.74	1.63	0.96	1.23	1.08

(E) *in crystallo* reaction of S113A Pol η with a dA-primer

	S113A+dA 0s	S113A+dA 40s	S113A+dA 80s	S113A+dA 140s	S113A+dA 230s	S113A+dA 300s
PDB Code	7M83	7M84	7M85	7M86	7M87	7M88
Data collection						
Space group	$P6_1$	$P6_1$	$P6_1$	$P6_1$	$P6_1$	$P6_1$
Cell dimensions						
a, b, c (Å)	98.30 98.30 81.83	98.10 98.10 82.13	98.36 98.36 81.75	98.16 98.16 82.51	98.26 98.26 81.93	98.32 98.32 81.94
α, β, γ (°)	90, 90, 120	90, 90, 120	90, 90, 120	90, 90, 120	90, 90, 120	90, 90, 120
Resolution (Å) [1]	85.27-1.55 (1.58-1.55)	29.93-1.47 (1.50-1.47)	25.97-1.75 (1.78-1.75)	29.94-1.55 (1.58-1.55)	30.00-1.85 (1.88-1.85)	29.97-1.66 (1.69-1.66)
R_{sym} or R_{merge} [1]	5.6 (58.2)	6.0 (67.6)	7.3 (77.1)	7.1 (68.1)	5.1 (57.3)	6.8 (65.9)
$I / \sigma I$ [1]	10.3 (2.2)	11.0 (2.5)	10.4 (2.1)	11.3 (2.2)	11.4 (2.1)	10.2 (2.3)
Completeness (%) [1]	96.5 (92.4)	99.9 (99.5)	95.9 (92.2)	99.8 (99.4)	99.6 (99.0)	99.2 (99.1)
Redundancy [1]	3.2 (2.6)	3.7 (3.5)	3.8 (3.3)	3.8 (3.7)	3.7 (3.5)	3.6 (3.4)
Refinement						
No. Reflections [1]	62856 (6018)	76205 (7564)	43376 (4115)	65424 (6491)	38238 (3748)	52529 (5207)
R_{work}	0.17 (0.25)	0.17 (0.24)	0.17 (0.25)	0.17 (0.22)	0.20 (0.29)	0.17 (0.24)
R_{free}	0.21 (0.28)	0.20 (0.28)	0.21 (0.31)	0.20 (0.25)	0.23 (0.35)	0.21 (0.28)
No. atoms	4524	4647	4621	4571	4577	4559
Macromolecules	3979	4062	4064	4008	4014	4015
Ligands	50	51	51	61	61	61
Solvent	495	534	506	502	502	483
B-factors	24.8	21.2	25.5	20.7	24.8	25.3
Macromolecules	24	20.3	24.7	19.6	24	24.6
Ligands	18.6	15.7	20.4	14.3	17.9	18.7
Solvent	32.1	28.5	32.1	29.5	31.9	32.7
Reaction						
Ratio of RS/PS	1.0 / 0	1.0 / 0	1.0 / 0	0.8 / 0.2	0.75 / 0.25	0.7 / 0.3
A-site	0.2 K^+	0.55 Mg^{2+}	0.65 Mg^{2+}	0.65 Mg^{2+}	0.65 Mg^{2+}	0.6 Mg^{2+}
A-site B-factor	18.8	13.8	19.2	13.3	14.1	15
B-site	1 Ca^{2+}	0.6 Ca^{2+} / 0.4 Mg^{2+}	0.5 Ca^{2+} / 0.5 Mg^{2+}	0.5 Ca^{2+} / 0.5 Mg^{2+}	0.5 Ca^{2+} / 0.5 Mg^{2+}	0.4 Ca^{2+} / 0.6 Mg^{2+}
B-site B-factor	12.9	8.5 / 8.6	11.3 / 11.7	8.1 / 8.3	10.1 / 9.9	11.5 / 11.5
C-site	-	-	-	0.2 Mg^{2+}	0.25 Mg^{2+}	0.3 Mg^{2+}
C-site B-factor	-	-	-	14.9	14.4	18.6
Ramachandran						
Favored (%)	97.7	97.7	97.4	97.4	97.4	97.2
Outlier (%)	0	0	0	0	0	0
R.m.s deviations						
Bond lengths (Å)	0.008	0.007	0.007	0.007	0.008	0.007
Bond angles (°)	1.15	1.08	1.04	1.15	1.08	1.03

(F) *in crystallo* reaction of S113A Pol η with an rA-primer

	WT+dA 0s	WT+dA 40s	WT+dA 140s	WT+dA 230s	WT+dA 300s
PDB Code	7M89	7M8A	7M8B	7M8C	7M8D
Data collection					
Space group	$P6_1$	$P6_1$	$P6_1$	$P6_1$	$P6_1$
Cell dimensions					
a, b, c (Å)	99.14 99.14 82.01	98.39 98.39 82.03	98.71 98.71 81.68	98.69 98.69 81.68	98.42 98.42 81.62
α, β, γ (°)	90, 90, 120	90, 90, 120	90, 90, 120	90, 90, 120	90, 90, 120
Resolution (Å) [1]	32.45-1.83 (1.86-1.83)	29.98-1.91 (1.94-1.91)	31.46-1.85 (1.88-1.85)	30.04-1.80 (1.83-1.80)	29.97-1.92 (1.95-1.92)
R_{sym} or R_{merge} [1]	7.9 (66.2)	7.7 (58.7)	7.4 (61.1)	6.8 (62.4)	8.4 (69.4)
I / σI [1]	10.3 (2.1)	8.9 (1.7)	12.3 (2.6)	14.0 (2.2)	11.6 (2.2)
Completeness (%) [1]	98.5 (98.3)	99.5 (99.1)	98.8 (97.3)	99.9 (99.5)	99.8 (99.9)
Redundancy [1]	3.2 (3.2)	2.7 (2.3)	4.1 (4.1)	3.8 (3.6)	3.7 (3.6)
Refinement					
No. Reflections [1]	39750 (3953)	34865 (3439)	38354 (3777)	41858 (4141)	34302 (3409)
R_{work}	0.17 (0.25)	0.17 (0.27)	0.16 (0.21)	0.17 (0.25)	0.16 (0.23)
R_{free}	0.21 (0.32)	0.22 (0.36)	0.21 (0.27)	0.20 (0.30)	0.22 (0.33)
No. atoms	4471	4543	4544	4554	4501
Macromolecules	3947	4000	4000	3998	3975
Ligands	50	60	61	61	61
Solvent	474	483	483	495	466
B-factors	26.4	28.8	27.6	27.8	28.5
Macromolecules	25.7	28.2	26.9	27	28
Ligands	26.2	25.9	23.4	24.8	26.6
Solvent	32.2	34.2	33.6	33.9	33.6
Reaction					
Ratio of RS/PS	0.85 / 0	0.4 / 0.45	0.3 / 0.55	0.25 / 0.6	0.2 / 0.65
A-site	0.2 K^+	0.3 Mg^{2+}	0.3 Mg^{2+}	0.25 Mg^{2+}	0.2 Mg^{2+}
A-site B-factor	31.3	26.5	20.8	20	27.4
B-site	0.85 Ca^{2+}	0.3 Ca^{2+} / 0.55 Mg^{2+}	0.15 Ca^{2+} / 0.7 Mg^{2+}	0.1 Ca^{2+} / 0.75 Mg^{2+}	0.85 Mg^{2+}
B-site B-factor	25.1	24.3 / 24.3	20.5 / 20.5	22.2 / 22.1	24.4
C-site	-	-	0.3 Mg^{2+}	0.4 Mg^{2+}	0.3 Mg^{2+}
C-site B-factor	-	-	22.9	*26.5*	25
Ramachandran					
Favored (%)	98.1	97.7	97.7	97.7	97.4
Outlier (%)	0	0	0	0	0
R.m.s deviations					
Bond lengths (Å)	0.006	0.006	0.006	0.008	0.006
Bond angles (°)	0.86	0.89	0.88	1.08	0.88

1. Data in the highest resolution shell is shown in the parenthesis.

Table S2. Oligonucleotides used in kinetic and crystallographic studies

	DNA template and primer	Pol η
Fig. 2A		
dA-primer	3′ CACGGATCGCATTTGTACTGAG 5′ GTGCCTAGCGTA**A**	WT or S113A
dT-primer	3′ CACGGATCGCATATGTACTGAG 5′ TGCCTAGCGTA**T**	WT or S113A
Fig. 4A and 6B		
dA, rA or 2′F-dA	3′ CACGGATCGCAT**T**TGTACTGAG 5′ TGCCTAGCGT**A** (dA, rA or 2′F-dA)	WT or S113A
dT or rU	3′ CACGGATCGCATATGTACTGAG 5′ TGCCTAGCGTA**T** (dT or rU)	S113A
Crystallization		
A-terminated primer	3′ TCGCAGTTTTAC 5′ AGCGTCA**A** (dA, rA or 2′F-dA)	WT or S113A
T-terminated primer	3′ TCGCAGTATTAC 5′ AGCGTCA**T**	S113A

SI References

1. S. French, K. Wilson, On the treatment of negative intensity observations. *Acta Crystallographica Section A* **34**, 517-525 (1978).
2. W. Kabsch, Xds. *Acta Crystallogr D* **66**, 125-132 (2010).
3. Z. Otwinowski, W. Minor, Processing of X-ray diffraction data collected in oscillation mode. *Method Enzymol* **276**, 307-326 (1997).
4. M. D. Winn *et al.*, Overview of the CCP4 suite and current developments. *Acta Crystallogr D* **67**, 235-242 (2011).
5. P. D. Adams *et al.*, PHENIX: a comprehensive Python-based system for macromolecular structure solution. *Acta Crystallogr D* **66**, 213-221 (2010).
6. P. Emsley, B. Lohkamp, W. G. Scott, K. Cowtan, Features and development of Coot. *Acta Crystallogr D* **66**, 486-501 (2010).
7. L. Schrodinger (2010) The PyMOL Molecular Graphics System, Version 1.3r1.
8. Y. Gao, W. Yang, Capture of a third Mg(2)(+) is essential for catalyzing DNA synthesis. *Science* **352**, 1334-1337 (2016).
9. S. Jo, T. Kim, V. G. Iyer, W. Im, CHARMM-GUI: a web-based graphical user interface for CHARMM. *J Comput Chem* **29**, 1859-1865 (2008).
10. R. B. Best *et al.*, Optimization of the additive CHARMM all-atom protein force field targeting improved sampling of the backbone phi, psi and side-chain chi(1) and chi(2) dihedral angles. *J Chem Theory Comput* **8**, 3257-3273 (2012).
11. J. Huang, A. D. MacKerell, Jr., CHARMM36 all-atom additive protein force field: validation based on comparison to NMR data. *J Comput Chem* **34**, 2135-2145 (2013).
12. J. Huang *et al.*, CHARMM36m: an improved force field for folded and intrinsically disordered proteins. *Nat Methods* **14**, 71-73 (2017).
13. T. Darden, D. Yark, L. Pedersen, Particle mesh Ewald: An N·log(N) method for Ewald sums in large systems. *J. Chem. Phys.* **98**, 10089-10092 (1993).
14. J.-P. Ryckaert, G. Ciccotti, H. J. C. Berendsen, Numerical integration of the cartesian equations of motion of a system with constraints: molecular dynamics of n-alkanes. *J. Comput. Phys.* **23**, 327-341 (1977).
15. P. Eastman *et al.*, OpenMM 7: Rapid development of high performance algorithms for molecular dynamics. *PLoS Comput Biol* **13**, e1005659 (2017).
16. B. R. Brooks *et al.*, CHARMM: the biomolecular simulation program. *J Comput Chem* **30**, 1545-1614 (2009).